Iranian Journal of Medical Physics

ijmp.mums.ac.ir

Determination of the Energy Windows for the Triple Energy Window Scatter Correction Method in Gadolinium-159 Single Photon Emission Computed Tomography Using Monte Carlo Simulation

Youssef Bouzekraoui[1], Farida Bentayeb[1], Hicham Asmi[1], Faustino Bonutti[2]

1. Laboratory of high energy physics and Monte Carlo simulation, Faculty of Sciences, University Mohammed V, Rabat, Morocco
2. Academic Hospital of Udine, Medical Physics Department, Italy

ARTICLE INFO

Article type:
Original Article

Article history:
Received: Oct 15, 2018
Accepted: Feb 25, 2019

Keywords:
Gd-159
Monte Carlo Simulation
Object Scatter
SPECT

ABSTRACT

Introduction: In radionuclide imaging, object scatter is one of the major factors leading to image quality degradation. Therefore, the correction of scattered photons might have a great impact on improving the image quality. Regarding this, the present study aimed to determine the main and sub-energy windows for triple energy window (TEW) scatter correction method using the SIMIND Monte Carlo simulation code in Gadolinium-159 (Gd-159) imaging.

Material and Methods: The energy window was set for various main energy window widths (i.e., 10%, 15%, and 20%) and sub-energy window widths (i.e., 3 and 6 keV). Siemens Medical System Symbia fitted with a high-energy collimator was used with Gd-159 point source positioned at seven locations inside the cylindrical water phantom. A comparison was made between the true primary to total ratio (calculated by SIMIND) and the primary to total ratio estimated using TEW method.

Results: The findings of this study showed that 20% of the main energy windows with 3 and 6 keV sub-energy windows were optimal for the implementation of the TEW method in Gd-159.

Conclusion: According to the results, the optimal energy windows for Gd-159 scintigraphy were the sub-energy windows of 3 and 6 keV. These findings could be helpful in the quantification of Gd-159 imaging.

► *Please cite this article as:*
Bouzekraoui Y, Bentayeb F, Asmi H, Bonutti F. Determination of Energy Windows for Triple Energy Window Scatter Correction Method in Gadolinium-159 Single Photon Emission Computed Tomography Using Monte Carlo Simulation. Iran J Med Phys 2019; 16: 405-409. 10.22038/ijmp.2019.34142.1429.

Introduction

In gamma camera imaging, the detection of Compton scattered photons within the photo-peak energy window depends on various factors, such as source distribution, object size, energy window settings, and source energies [1-3]. On the other hand, the removal of scattered photons is important in improving the quality and quantity of image [4] because only primary photons provide correct spatial information regarding radioisotope distribution [5].

Diverse methods have been proposed to eliminate scattered photons from planar or reconstructed images, namely dual-energy window (DEW) [6], triple-energy window (TEW) [7], photopeak window [8], downscatter correction [8], and combined scatter correction [8]. Some other methods for this purpose include deconvolution [9], energy-weighted acquisition [10], iterative peak-erosion algorithm, spectral-fitting algorithm [11], factor analysis [12], inverse Monte Carlo reconstruction algorithm [13], and asymmetric photopeak window (offset high) [14].

The Gadolinium-159 (Gd-159) isotope can be used for nuclear medicine due to its half-life (18.5 h), in addition to beta (1001 keV) and gamma (main energy of 363.54 keV) emissions [15, 16]. In order to enhance the activity quantification and image quality for Gd-159 using the gamma emission of 365.54 keV, it is important to correct the scatter events caused by the photons scattered in the object. These photons produce errors regarding the decay location.

This study aimed to estimate the contribution of scattered photons inside the main energy window in the TEW method [17-26], which is known as a simple and practical technique. In the TEW method, two sub-windows were placed on both sides of the main photo-peak window. The primary count of photons in the photo-peak was calculated using the counts acquired from the two adjacent narrow windows.

The current study involved the comparison of the true primary to total ratio and primary to total ratio (estimated by TEW) using the SIMIND Monte Carlo simulation code [27]. The results could be beneficial

**Corresponding Author:* Tel: +212670949767; Email: youssef0fsr@gmail.com

for determining the main and sub-energy windows in Gd-159 SPECT imaging.

Materials and Methods

The SIMIND Monte Carlo code (version 6.1) was used to simulate the Siemens Symbia Medical gamma camera with high-energy (HE) collimators that have parallel holes (Table 1). The dimensions of the detector surface were 59.1×44.5 and had a NaI (Tl) crystal thickness of 2.54 cm. The detector was characterized by an intrinsic spatial resolution of 0.34 cm and energy resolution of 8.8% at 140 keV. The photons emitted toward the camera had an acceptance angle of 45°. The pixel size in the simulated planar source images was 0.34 cm with a matrix size of 128×128 cm. The binary images were imported to the ImageJ software developed by SIMIND.

Table 1. Characteristics of the Siemens Symbia medical system collimator

Low energy	High-energy (HE) collimator
Hole geometric	Hexagonal
Hole length (cm)	5.97
Septal thickness (cm)	0.2
Hole diameter (cm)	0.4

We simulated a cylindrical water phantom (16 cm in diameter and 32 cm in height) positioned at a distance of 15 cm from the detector surface. Point sources with a diameter of 1 mm, filled with Gd-159 (3,7 MBq), were simulated at seven locations, including the center of the cylinder phantom, as well as offsets at ±7 cm of X, Y, and Z directions relative to the center. Figure 1 depicts the geometry of the SPECT system and phantom used in this study.

The main energy window was determined at the widths of 10%, 15%, and 20%, while centered at 363 keV and the sub-energy window widths of 3 and 6 keV. The true primary to total ratio (P/T) was compared with the primary to total ratio estimated using TEW scatter-correction method with triangular approximation.

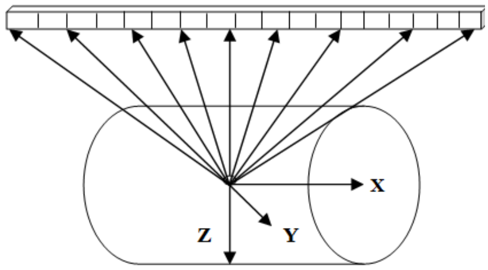

Figure 1. Geometry of the single photon emission computed tomography system and phantom

The count of primary photons for photopeak was estimated with the main window centered at the photopeak energy window and the two sub-windows on the sides of the main window. The following equation was used to estimate the scatter counts:

$$C_{sca} = \left(\frac{C_{left}}{W_s} + \frac{C_{right}}{W_s}\right) \times \frac{W_m}{2} \quad (1)$$

$$C_p = C_{tot} - C_{sca} \quad (2)$$

Where, C_{left} denotes the counts in left lower sub-energy window, C_{right} represents the counts in right lower sub-energy window, W_s is the width of sub-energy window, W_m refers to the width of main window, C_{tot} signifies the counts in main window, C_{sca} is the scatter counts, and C_p represents the primary counts.

In addition, the primary to total ratio was calculated as:

$$P/T = \frac{C_p}{C_{tot}} \times 100 \quad (3)$$

Results

Tables 2 and 3 show the difference between the true primary to total ratio (%) and the estimated primary to total ratio at each position for 3 and 6 keV sub-windows. The primary to total ratio of photons depended on the source location and energy windows

Table 2. Difference between the true primary to total ratio (%) and primary to total ratio estimated by triple-energy window scatter correction method for sub-window 3

Subwin (3 keV)	10%		15%		20%		10%	15%	20%
Source position (x, y, z)	P/T TEW	P/T true	P/T TEW	P/T true	P/T TEW	P/T true	Difference (%)	Difference (%)	Difference (%)
(0, 0, 0)	88.05	85.4	88.4	80.2	82.17	75.36	2.65	8.2	6.82
(-7, 0, 0)	90.34	84.2	84.43	79.3	80.25	74.11	6.14	5.13	6.14
(7, 0, 0)	89.56	85.7	88.71	80.4	83.38	75.53	3.86	8.31	7.85
(0, -7, 0)	94.13	92.5	90.02	89.2	88.22	86.32	1.63	0.82	1.9
(0, 7, 0)	92.55	92.1	90.28	88.6	87.78	85.6	0.45	1.68	2.18
(0, 0, -7)	83.73	76.5	82.35	69.1	76.66	63.27	7.23	13.25	13.39
(0, 0, 7)	93.79	97.4	91.88	96.5	92.57	95.19	-3.61	-4.62	-2.62

Table 3. Difference between the true primary to total ratio (%) and primary to total ratio estimated by triple-energy window scatter correction method for sub-window 6

Subwin (6 keV)	10%		15%		20%		10%	15%	20%
Source position (x, y, z)	P/T TEW	P/T true	P/T TEW	P/T true	P/T TEW	P/T true	Difference (%)	Difference (%)	Difference (%)
(0, 0, 0)	75.85	85.4	75.6	80.2	66.25	75.4	-9.55	-4.6	-9.15
(-7, 0, 0)	81.16	84.2	68.07	79.3	65.18	74.1	-3.04	-11.23	-8.92
(7, 0, 0)	77.57	85.7	76.12	80.4	66.32	75.5	-8.13	-4.28	-9.18
(0, -7, 0)	86.67	92.5	80.99	89.2	78.13	86.3	-5.83	-8.21	-8.17
(0, 7, 0)	84.63	92.1	81.65	88.6	76.03	85.6	-7.47	-6.95	-9.57
(0, 0, -7)	67.85	76.5	63.82	69.1	55.26	63.3	-8.66	-5.28	-8.04
(0, 0, 7)	89.48	97.4	85.61	96.5	86.94	95.2	-7.92	-10.89	-8.26

Table 4. Gadolinium-159 point sources obtained for the sub-windows of 3 keV and a main energy window of 10%

Source position (x, y, z)	True primary images	Primary images (TEW)	Total images
(0, 0, 0)	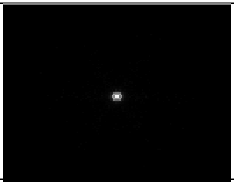	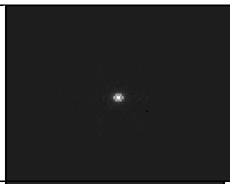	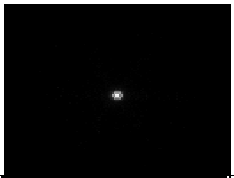
(-7, 0, 0)	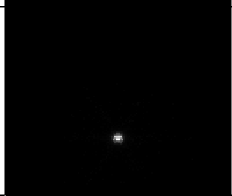	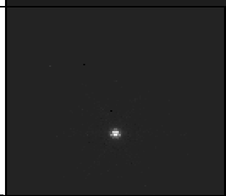	
(7, 0, 0)	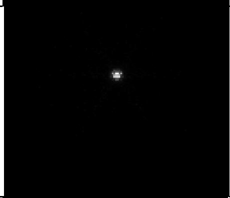		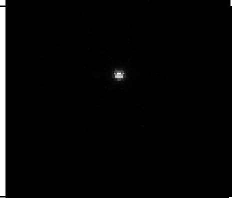
(0, -7, 0)	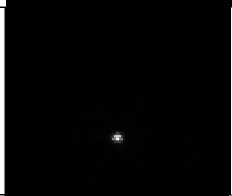		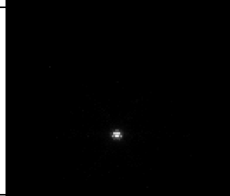
(0, 7, 0)	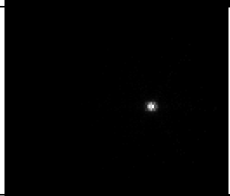	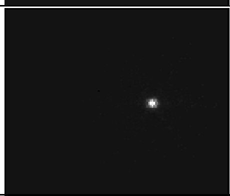	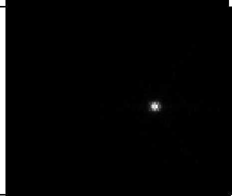
(0, 0, -7)	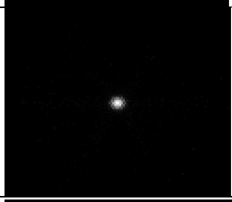	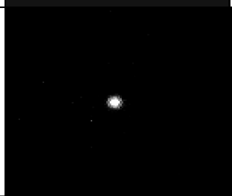	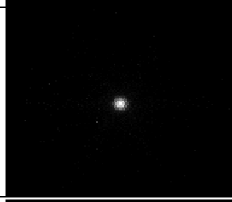
(0, 0, 7)	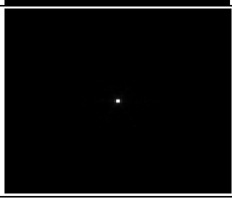	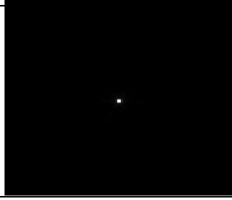	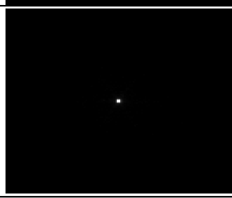

Discussion

Gadolinium-159 as a beta emitter is an efficient radionuclide for cancer therapy [28-31]. Therapeutic management requires quantitative imaging, which is difficult to perform due to several factors, such as object scatter. Previous studies on the proprieties of therapeutic and scintigraphic images with Gd-159 demonstrated that the images obtained with a high-energy general-purpose collimator possessed low quality [16, 29].

The scatter correction methods are useful to improve the image quality and activity quantification. Noori-Asl et al. [24] evaluated and compared six scatter correction methods for SPECT Tc-99m spectrum using SIMIND Monte Carlo simulation. They introduced TEW method, considering triangular approximation, as the most proper correction procedure.

However, there is no study regarding the fraction of Gd-159 scattered photons as the function of optimal main and sub-energy windows for the implementation of the TEW method. Selection of the optimal main and sub-energy windows is very important and can lead to suitable image quality. Therefore, the selection of the main and sub-energy windows was different in Gd-159 SPECT imaging. It is important to choose proper energy windows for avoiding the scattered photons that degrade quantification and image quality. As a result, the chosen main and sub-energy windows impose a great effect on scatter correction for Gd-159 SPECT imaging.

In the current study, it was shown that the detected scattered photons within photo-peak energy window highly depended on the size of source distribution and energy window parameters. The use of SIMIND Monte Carlo simulation code facilitates tracking and recording the life history of the individual photon originating from the source. This allows the accurate calculation of the scattered photon fractions in different energy windows. The TEW scatter correction method was easily executed in the clinical trial.

Conclusion

The present study evaluated the TEW scatter correction method for Gd-159 imaging with SIMIND Monte Carlo simulation code. The obtained results showed that both 3 and 6 keV sub-windows with 10% main-energy window were optimum for implementing the TEW method. These findings might be helpful in the activity quantification of Gd-159. Moreover, the capacity of quantitative SPECT imaging was shown using the TEW scatter correction method. The results of this study shed light on Gd-159 radionuclide as a new privileged radionuclide in the treatment and diagnosis of cancer.

References

1. Ogawa K, Harata Y, Ichihara T, Kubo A, Hashimoto S. Estimation of scatter component in SPECT planar image using a Monte Carlo method. Jpn J Nucl Med. 1990; 27: 467-75.
2. Floyd CE, Jaszczak RJ, Harris CC, Coleman RE. Energy and spatial distribution of multiple order Compton scatter in SPECT: a Monte Carlo simulation. Phys Med Biol. 1984; 29:1217-30.
3. Floyd CE, Jaszczak RJ, Coleman RE. Inverse Monte Carlo: A Unified Reconstruction Algorithm for SPECT. IEEE Trans Nucl Sci.1985; 32: 779-85.
4. Sadremomtaz A, Telikani Z. Evaluation of the performance of parallel-hole collimator for high resolution small animal SPECT: A Monte Carlo study. Iran J Nucl Med. 2016; 24(2):136-43.
5. Razavi SH, Kalantari F, Bagheri M, Namiranian N, Nafisi-Moghadam R , Mardanshahi A, et al. Characterization of low, medium and high energy collimators for common isotopes in nuclear medicine: A Monte Carlo study. Iran J Nucl Med. 2017; 25(2):100-4.
6. Jaszczak RJ, Greer KL, Floyd CE Jr, Harris CC, Coleman RE. Improved SPECT quantification using compensation for scattered photons. J Nucl Med.1984; 25:893‑900.
7. Ogawa K, Harata Y, Ichihara T, Kubo A, Hashimoto S. A practical method for position-dependent Compton-scatter correction in single photon emission CT. IEEE Trans. Med. Imaging. 1991; 10: 408.
8. Lagerburg V, de Nijs R, Holm S, Svarer C. A comparison of different energy window subtraction methods to correct for scatter and down scatter in I-123 SPECT imaging. Nucl Med Commun. 2012; 33(7):708-18.
9. Axelsson B, Msaki B, Israelsson A. Subtraction of Compton scattered photons in single-photon emission computerized tomography. J Nucl Med. 1984; 25: 490-4
10. Hamill JJ, DeVito RP. Scatter reduction with energy weighted acquisition. IEEE Trans Nucl Sci.1989; 36: 1334-9.
11. Koral KF, Wang X, Rogers WL, Clinthorne NH, Wang X. SPECT Compton-scattering correction by analysis of energy spectra. J Nucl Med. 1988; 29: 195-202.
12. Gagnon D, Todd-Pokropek AE, Arsenault A, Dupras G. Introduction to holospectral imaging in nuclear medicine for scatter subtraction. IEEE Trans Med Imag. 1989; 8: 245-50.
13. 13- Floyd CE, Jaszczak RJ, Coleman RE. Scatter detection in SPECT imaging: dependence on source depth, energy, and energy window. Phys Med Biol. 1988; 33:1075-81.
14. Koral KF, Clinthorne NH, Rogers WL. Improving emission-computed-tomography quantification by Compton-scatter rejection through offset window. Nucl Inst and Methods in Phys Res A. 1986; 242: 610-4.
15. Soares DCF, Menezes MA de BC, dos Santos RG, Ramaldes GA. Gd-159: preparation and preliminary evaluation asa potential antitumoral radionuclide. J Radioanal Nucl Chem. 2010; 284: 315-20.
16. Soares DCF, Sousa GFD, Barros ALBD , Cardoso VN, Oliveira MCD , Ramaldes GA. Scintigraphic imaging and increment in mice survival using theranostic liposomes based on Gadolinium-159. J of Dru Del Science and Tech. 2015; 30:7-14.
17. Lee YS, Kim JS, Kim KM, Lima SM , Kimb HJ. Determination of energy windows for the triple energy window scatter correction method in I-131

on a Siemens SYMBIA gamma camera: a GATE simulation study. J of Inst. 2015; 10:1-8.
18. Takayama T, Ichihara T, Motomura N, Ogawa K. Determination of Energy Window Width and Position for Scintigraphic Imaging Using Different Energy Resolution Detection with the 'Triple Energy Winddw (TEW) Scatter Compensation Method. IEEE. 1998; 35(2):51-9.
19. Changizi V, Takavar A, Babakhani A, Sohrabi M. Scatter correction for heart SPECT images using TEW method. J Appl Clin Med Phys. 2008; 9(3):2767.
20. Dewaraja Yk, Ljungberg M, Fessler JA. 3-D Monte Carlo-based scatter compensation in quantitative I-131 SPECT reconstruction. IEEE Trans Nucl Sci. 2006; 53:181-8.
21. Dewaraja Yk. Quantitative 131I SPECT with triple energy window Compton scatter correction. IEEE Trans. Nucl. Sci. 1998; 45:3109.
22. Ljungberg M, King MA, Hademenos J, Strand SE. Comparison of four scatter correction methods using Monte Carlo simulated source distribution. J Nucl Med. 1994; 35:143-51.
23. Fujioka H, Inoue T, Ishimaru Y, Akamune A, Murase K, Tanada S, et al. Compton scatter correction using the triple energy window (TEW) method in conventional single photon emission computed tomography without TEW acquisition hardware. Kaku Igaku. 1997; 34(4):251-8.
24. Ogawa K. Simulation study of triple-energy-window scatter correction in combined TI-201, Tc-99m SPECT. Ann of Nucl Med. 1994; 8(4):277-81.
25. Takahashi A, Himuro K, Yamashita Y, Komiya I, Baba S, Sasaki M. Monte Carlo simulation of PET and SPECT imaging of 90Y. Med Phys. 2015; 42(4):1926-35.
26. Noori-Asl M, Sadremomtaz A, Bitarafan-Rajabi A. Evaluation of three scatter correction methods based on estimation of photopeak scatter spectrum in SPECT imaging: a simulation study. Phys Med. 2014; 30(8):947-53.
27. Ljungberg M. The SIMIND Monte Carlo program Home Page. Available from: https://www.msf.lu.se/forskning/the-simind-monte-carlo-program.
28. Soares DCF, Oliveira MCD, Santos RGD, Andrade MS, Vilela JMC, Cardoso VN, et al. Liposomes radiolabeled with 159Gd-DTPA-BMA: Preparation, physicochemical characterization, release profile and in vitro cytotoxic evaluation. Eur J Pharm Sc. 2011;42: 462‑9.
29. Soares DCF, Oliveira MCD, Barros ALBD, Cardoso VN, Ramaldes GA. Liposomes radiolabeled with 159Gd: In vitro antitumoral activity, biodistribution study and scintigraphic image in Ehrlich tumor bearing mice. Eur J Pharm Sc. 2011. 43:290‑6.
30. Galvão I, Santos RG, Neves MJ. Evaluation of Gd and Gd159 as new approaches for cancer treatment. Inter Nucl Atl Conf. 2011;24-8.
31. Cipreste MF, Peres AM, Cotta AAC, AragonFH, Antunes ADM, Leal AS, et al. Synthesis and characterization of 159Gd-doped hydroxyapatite nanorods for bioapplications as theranostic systems. Mat Chem Phy. 2016; 181:301-11.